

Vestian Reflectance Spectral Characteristic Map Based on Unsupervised Classification of Multiband Reflectance Data Obtained by DAWN Framing Camera and Its Relation of Chemical Composition and Topographic Features. Yoshiaki Ishihara¹, Makoto Hareyama², and Makiko Ohtake³, ¹Sattelite Observation Center, National In-stitute for Environmental Studies (ishihara.yoshiaki@nies.go.jp), ²St. Marianna University School of Medicine. ³Institute of Space and Astronautical Science, Japan Aerospace Exploration Agency

Introduction: The 4 Vesta is the third-largest minor body and is thought like the differentiated rocky inner planets. Remote-sensing data indicates that 4 Vesta is a differentiated body consisting of at least three distinct layers (crust, mantle, and core). Compositional information about 4 Vesta is based on ground-based and Hubble Space Telescope (HST) spectroscopic observations, as well as lab analyses of Howardite-Eucrite-Diogenite (HED) meteorites, which are probably impact-produced fragments of Vesta [1, 2]. Furthermore, in this decade, the new Vestian dataset was added by in-situ remote-sensing by NASA's DAWN mission. Therefore, 4 Vesta is the best examples for studying the origins and evolution of rocky-proto-planetary bodies and terrestrial planetary bodies during the first 10 million years after the solar system formation.

The global geologic map of 4 Vesta is fundamental and important for understanding the formation of Vestian internal structures and crustal evolution. The Dawn dataset, such as Framing Camer (FC) [3] enables us to create a global geologic map with high spatial resolution and could be compared with a distribution of chemical composition and/or topographic features observed by other instruments onboard DAWN. As a first step, we

made a global spectral feature classification map. Although 4 Vesta is an asteroid, it is still too big to classify the whole surface by fully manual processing. We, therefore, try to use some machine learning base methods (i.e. unsupervised classification). Recently, such automatic classification was adopted to lunar datasets and it worked well [4]. The spectral data used this study is FC High Altitude Mapping Orbit (HAMO) color mosaic (DAWN-A-FC2-5-MOSAIC-V1.0, spatial resolution 60 m/pixel, and those spectral wavelengths are 438, 555, 653, 749, 829, 917, and 965nm [1]) (Figs. 1, 2).

These FC's seven spectral bands enable us to distinguish between the eucritic (pyroxene-plagioclase basalts) and diogenitic (ortho-pyroxenites) dominated lithologies, and these lithologies thought to probably consist on Vestian surface. This work compares the global spectral classification map with chemical composition maps and topographic features and discusses the relation between spectral features and chemical composition and topographic features on the Vestian surface.

Classification and average spectra: The data classified in this study are seven bands cubed global mosaic data called HAMO mosaic of DAWN/FC. This

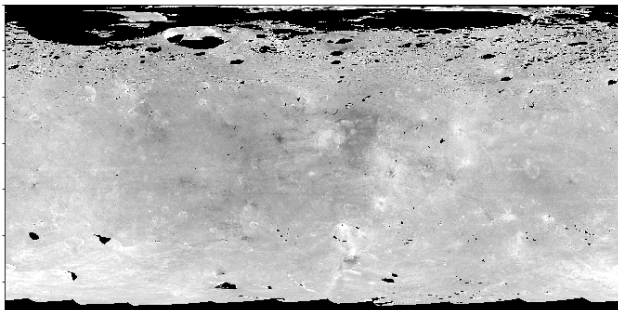


Fig. 2 FC 749 nm band reflectance map of the 4 Vesta

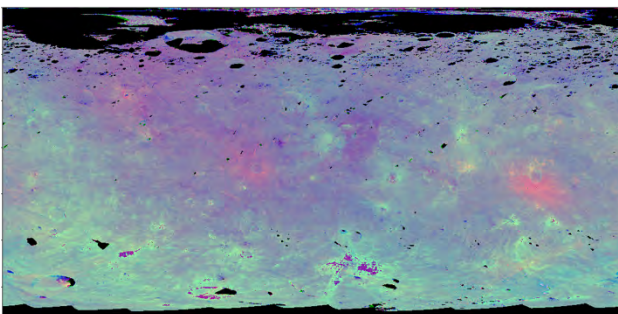


Fig. 1 FC global color mosaic of the 4 Vesta (R = 749/438 nm, G = 749/917 nm, and B = 438/749 nm).

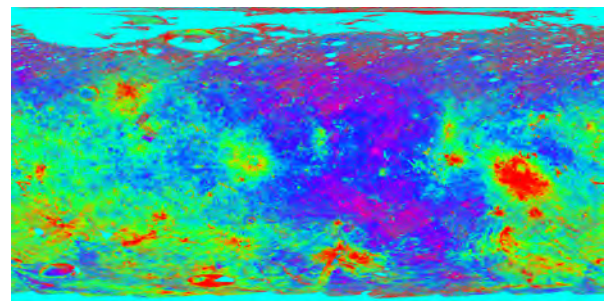


Fig. 3 Principal Component 7 Map for FC HAMO color mosaic data

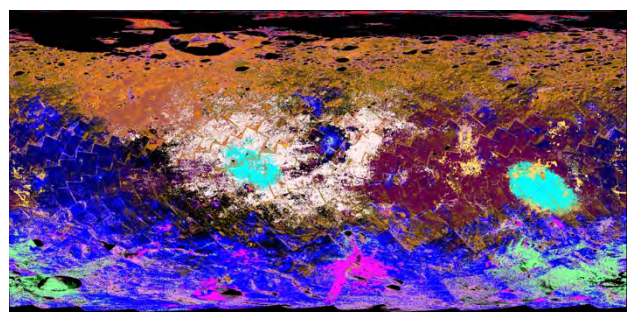


Fig. 4 Classification results of VGMM (n_class = 20)

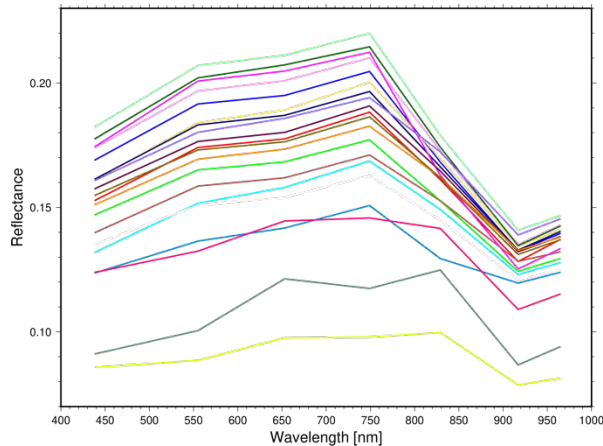


Fig. 5 Average Reflectance Spectrum of Each Class. Line Colors correspond to Fig. 4.

work analyzed the entire Vestian surface. Also, to suppress the albedo-related component of the spectra and capture the tiny spectral features, Principal Component Analysis (PCA) was adopted, and resulting normalized PCs were classified by Gaussian Mixture Model (GMM) and Variational Bayesian Gaussian Mixture Model (VBGMM) [5]. GMM only requires the number of classes as a priori knowledge. VBGMM is a fully unsupervised method and not require any prior information, even the number of classes.

The classification map (Fig. 4) correlates well with the color mosaic map (Fig. 2) and presents some collocated features with the PC7 map (Fig. 3). This suggests that the classification reflects both the albedo difference and the mineralogical difference of Vestian surface for each region. The mean reflectance spectrum of each class is shown in Fig. 5. The overall features of the mean spectrum of each class are quite similar (i.e., all mean spectra have minimum reflectance at 917 nm), but those have captured the differences of weak absorption around the 600nm band, the pseudo-depth of the 1 μm absorption band and the pseudo-band-minimum of 1 μm absorption. These differences reflect the mafic mineral type, in other words, the difference of HED meteorite type.

Comparison to elemental distribution and Topographic features: Comparing the classification map with other kinds of datasets, such as topographic structures [6] (Fig. 6) and hydrogen concentration derived from GRD data [7] (Fig. 7), we have found weak correlation of broad scale structure of between hydrogen concentration and classification results in equatorial region, and we also found in and around some large craters located in southern hemisphere classified as different spectral class of surrounding area. These craters located in more large basin, and so will be

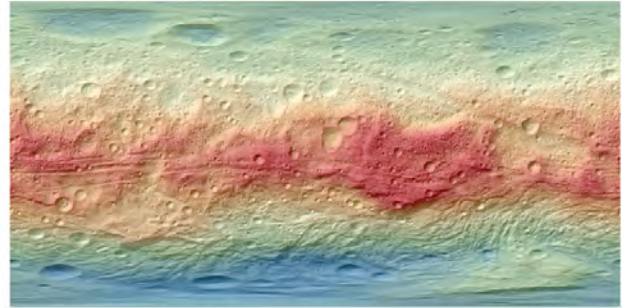


Fig. 6 Shaded Topography [6]

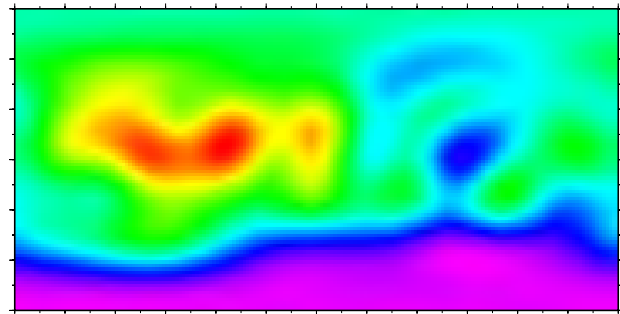


Fig. 7 Hydrogen Concentration [7]. Red indicates the highest and purple indicates the lowest concentration.

excavates very deep materials, so these distinct class probably reflects Vesta's differentiated internal structure, and careful interpretation of the average spectrum and depth information is necessary.

Conclusion: The reflectance spectra of the 4 Vesta have been classified globally by unsupervised methods. Although the average spectra are quite similar for most classes, small differences were captured the 600 nm band and 1 μm absorption shape and depth, those reflect the mafic mineral type. Also, the classification result shows a few craters in southern hemisphere possess different class compared with around the region. This probably shows that the deep materials expose at these craters.

References: [1] Kel, K. (2002) in *Asteroids III*, 573-584. [2] McSween et al. (2011) *Space Sci. Rev.* 163, 141-174. [3] Sierks, H. et al. (2011) *Space Sci. Rev.* 163, 263-327. [4] Hareyama et al. (2019) *Icarus* 321, 407-423. [5] Ishihara et al. (2018) 49th LPSC, Abstract #1216. [6] Preusker, F. et al. (2014) 45th LPSC, Abstract #2027. [7] Prettyman, T.H. et al. (2012) *Science* 338(6104), 242-246.

Acknowledgements: This study is supported by JSPS KAKENHI (Grant-in-Aid for Scientific Research(C)) Grant Number 17K05644 (P.I.: Yoshiaki Ishihara).